Earth and Planetary Science Letters 563 (2021) 116870

Contents lists available at ScienceDirect

Earth and Planetary Science Letters

www.elsevier.com/locate/epsl

Event-dominated transport, provenance, and burial of organic carbon in the Japan Trench

T. Schwestermann [a,*], T.I. Eglinton [b], N. Haghipour [b,c], A.P. McNichol [d], K. Ikehara [e], M. Strasser [a,f]

[a] Institute of Geology, University of Innsbruck, Innrain 52, 6020 Innsbruck, Austria
[b] Geological Institute, ETH Zürich, Sonneggstrasse 5, 8092 Zürich, Switzerland
[c] Laboratory of Ion Beam Physics, ETH Zürich, Otto-Stern-Weg 5, 8093 Zürich, Switzerland
[d] Woods Hole Oceanographic Institution, National Ocean Sciences Accelerator Mass Spectrometry Facility, Woods Hole, MA 02543-1539, United States
[e] Geological Survey of Japan, National Institute of Advanced Industrial Science and Technology (AIST), Tsukuba Central 7, 1-1-1 Higashi, Tsukuba 305-8567, Japan
[f] MARUM – Center for Marine Environmental Sciences, University of Bremen, Leobener Str. 8, 28359 Bremen, Germany

ARTICLE INFO

Article history:
Received 10 June 2020
Received in revised form 7 November 2020
Accepted 1 March 2021
Available online 24 March 2021
Editor: Y. Asmerom

Keywords:
carbon isotopes
carbon provenance
hadal zone event-stratigraphy
carbon transfer
Japan Trench
ramped Pyr/Ox

ABSTRACT

The delivery of organic carbon (OC) to the ocean's deepest trenches in the hadal zone is poorly understood, but may be important for the carbon cycle, contain crucial information on sediment provenance and event-related transport processes, and provide age constraints on stratigraphic sequences in this terminal sink. In this study, we systematically characterize bulk organic matter (OM) and OC signatures (TOC/TN, $\delta^{13}C$, ^{14}C), as well as those from application of serial thermal oxidation (ramped pyrolysis/oxidation) of sediment cores recovered along an entire hadal trench encompassing high stratigraphic resolution records spanning nearly 2000 years of deposition. We analyze two cores from the southern and northern Japan Trench, where submarine canyon systems link shelf with trench. We compare results with previously published data from the central Japan Trench, where canyon systems are absent. Our analyses enable refined dating of the stratigraphic record and indicate that event deposits arise from remobilization of relatively surficial sediment coupled with deeper erosion along turbidity current pathways in the southern and central study site and from canyon flushing events in the northern study site. Furthermore, our findings indicate deposition of predominantly marine OC within hemipelagic background sediment as well as associated with event deposits along the entire trench axis. This implies that canyon systems flanking the Japan Trench do not serve as a short-circuit for injection of terrestrial OC to the hadal zone, and that tropical cyclones are not major agents for sediment and carbon transfer into this trench system. These findings further support previous Japan Trench studies interpreting that event deposits originate from the landward trench slope and are earthquake-triggered. The very low terrestrial OC input into the Japan Trench can be explained by the significant distance between trench and hinterland (>180 km), and the physiography of the canyons that do not connect to coast and river systems. We suggest that detailed analyzes of long sedimentary records are essential to understand OC transfer, deposition and burial in hadal trenches.

1. Introduction

Although it has been more than half a century since the pioneering work of sampling and analyzing organic carbon (OC) content of surface sediments in deep-water hadal trenches (water depths of >6000 m; Jumars and Hessler (1976); Bartlett (2009)), the processes involved in the transport, deposition and burial of OC in oceanic trenches remain poorly understood. Nevertheless, the supply of OC to the hadal zone is considered to play an important role in the deep-marine carbon cycle and in supporting hadal ecosystems (e.g., Jamieson et al., 2010; Kioka et al., 2019a; Nunoura et al., 2015). Detailed investigation on the quantification of OC mineralization and burial in the typically narrow and elongated oceanic trenches that comprise this terminal sedimentary sink have only recently emerged, owing to latest technological advances that allow for sampling and studying the sea- and subseafloor in such extreme water depths (e.g., Bao et al., 2018b, 2019; Glud et al., 2013, 2021; Leduc et al., 2016; Luo et al., 2017, 2018; Wenzhöfer et al., 2016). It has been documented that mi-

* Corresponding author.
E-mail address: tobisch91@bluewin.ch (T. Schwestermann).

https://doi.org/10.1016/j.epsl.2021.116870

crobial biomass, phytopigment concentrations, and infaunal abundances as well as benthic carbon mineralization rates are higher in the trench than their adjacent abyssal plain (e.g., Glud et al., 2013, 2021; Leduc et al., 2016; Luo et al., 2019). However, the remobilization processes and sediment and OC fluxes to trench environments that sustain hadal ecosystems are currently poorly constrained.

It has been speculated that because of their geometry and propagating internal tides, OC is funneled towards the trench bottom (Turnewitsch et al., 2014). However, recent observations in isolated trench basins or in canyons that connect coastal areas to deep-water trenches indicate that event-related sediment-gravity flows triggered by tropical cyclones or earthquakes have the potential to transfer, deposit and eventually bury vast amounts of OC in oceanic trenches (e.g., triggered by the 2008 Typhoon Morakot offshore Taiwan (e.g., Kao et al., 2010), the 2016 Kaikoura earthquake offshore New Zealand (Mountjoy et al., 2018); or the 2011 Tohoku-oki earthquake offshore Japan (Kioka et al., 2019a)). There is a need for improved understanding of carbon transfer to hadal trenches, including possible transport pathways (e.g., canyons, currents, gravitational slope processes) and trigger mechanisms that facilitate episodic OC transfer from the slope, shelf, or the terrestrial hinterland. An important and frequently proposed trigger mechanism along subduction trenches is earthquake, which can remobilize clastic materials and OC from the open adjacent slope and along canyons incising the slope (e.g., Bao et al., 2018b; Kioka et al., 2019a,b; Migeon et al., 2017). The resulting earthquake related event-deposits in the trench often consist of reworked marine sediments with varying contributions of terrestrial and volcanoclastic components and OC, depending on the geology and physiography of the subduction margin (e.g., Pouderoux et al., 2014; Ikehara et al., 2016; Goldfinger, 2009; Schwestermann et al., 2020). Tropical cyclones also serve as important trigger mechanisms to initiate sediment gravity flow and associated OC transport, especially when canyons connect trench basins with the coast and fluvial systems (e.g., Kao et al., 2010; Pope et al., 2017). Storm- and flood-induced event deposits in the deep-sea have been detected by the presence of terrestrial plant remains, such as leaves or wood fragments (Kao et al., 2010; Migeon et al., 2017). However, if macroscopic plant remains are absent, further geochemical analysis, such as determining the ratios of total OC to total nitrogen (TOC/TN) and carbon isotopic compositions of OC, is necessary to determine the provenance of OC and infer the dominant driving mechanism. Kao et al. (2010), for instance, reported for the Manila Trench (MT) that a deep-marine event deposit from a typhoon-flood triggered hyperpycnal flow has very similar isotopic values as the river sediments. Studies in the New Britain Trench (NBT; Luo et al., 2019; Xiao et al., 2020) show overall a high deposition of terrestrial OC in the trench (comprising 61±1% of the TOC) due to the steep landward trench slope (~8°) and the proximity to land (~60 km).

Above-mentioned studies cover different time-scales as they either examine known events captured by instrumental data (e.g., sediment traps: Kao et al., 2010; differential bathymetry: Mountjoy et al., 2018) or integrate data from dated surface cores encompassing the recent past (<100 years; Luo et al., 2019; Xiao et al., 2020). However, little is known about how the provenance and fluxes of OC vary over longer time scales that potentially span depositional episodes in response to different trigger processes that may have different recurrence rates (e.g., subduction-zone earthquakes occur at a lower frequency than tropical cyclones). Therefore, down-core studies covering event deposits that have occurred over several cycles of potential triggers (earthquakes, typhoons) are needed. For time scales beyond ^{210}Pb dating, however, it is challenging to date hadal stratigraphic records of sediments deposited far below the carbonate compensation depth (CCD) (Jamieson et al., 2010; Berger et al., 1976), which leads to the dissolution of dateable calcareous fossils. In areas where calcareous fossils are absent, ^{14}C dating of bulk OC and, more recently, thermal fractions from serial thermal oxidation (so-called ramped pyrolysis/oxidation, RPO) of OC have been applied to provide age constraints on stratigraphic sequences (e.g., Bao et al., 2018b; Subt et al., 2016; Rosenheim et al., 2008).

Pioneering hadal zone research investigating OC ^{14}C signatures has been undertaken in the central Japan Trench (JT; 7-8 km deep, offshore NE Japan; Fig. 1), where no canyons reaching the hadal zone incise the shelf or connect to rivers draining the hinterland. Extensive effort has been invested to understand sediment and carbon delivery to the trench linked to the 2011 Magnitude 9 Tohoku-oki earthquake (Bao et al., 2018b; Kioka et al., 2019a). Also, older earthquake-triggered event deposits that correlate to a 1300-year long history of megathrust earthquakes (Ikehara et al., 2016) exhibit bulk OC ^{14}C ages that are 3-6 kyr older compared to the respective under- and overlying hemipelagic background sediment (Bao et al., 2018b). The hemipelagic background strata show a robust linear relationship with sediment depth, although the age offset to known marker beds is ~1.6 kyr. Similar linear relationship and age-offset for intra-event stratigraphic successions was also observed in cores from the southern and northern JT (Kioka et al., 2019b), where the hadal trench, in contrast to the central JT, is connected to shallower waters by the Nakaminato and Ogawara canyon systems, respectively.

The Nakaminato canyon is potentially fed by the Naka and Tone rivers, the latter comprising the largest drainage area in Japan. The catchment areas of both rivers can be impacted by severe tropical cyclones, as occurred by the 2019 Faxai and Hagibis typhoons and the AD 1856 Edo-Ansei typhoon that is considered as one of the strongest typhoons in Japanese history (Sakazaki et al., 2015).

Thus, the hadal JT provides an ideal study site to investigate temporal and spatial variability in carbon provenance and transfer processes associated with event-related deposition in hadal trenches on a margin-wide scale. In this study, we analyzed two 10 m long sediment cores from terminal sinks of the Nakaminato and Ogawara canyons in the southern and northern JT, respectively. In order to assess carbon transfer through canyon systems versus open slope lateral remobilization and translocation processes, we compare results from these two cores with published data from the central JT (Bao et al., 2018b), where canyons are absent. We further examined the characteristics of surficial sediments on the adjacent landward slope. Through this comparison between different trench-fill basins and between trench bottom and trench slope settings, we seek to (1) constrain the provenance of OC along the entire JT (marine vs terrestrial OC), (2) to infer trigger mechanisms of event deposits (e.g., tropical cyclones vs. earthquakes), (3) to investigate the influence of sediment remobilization and redistribution processes on bulk OC ^{14}C characteristics of hadal trench sediments (e.g., hydraulic particle sorting; cf. Bao et al., 2019; Hemingway et al., 2019, and (4) to refine ^{14}C-based age models for JT sedimentary records.

2. Japan Trench (JT)

The JT subduction zone is located East of Honshu, Japan, where the Pacific Plate subducts beneath the Okhotsk Plate. Due to relatively high convergence rates of ~86 mm/a (DeMets et al., 2010) the area is frequently affected by strong earthquakes (e.g., the 2011 M_w9.0 Tohoku-oki earthquake). The trench is aligned along a NNE-SSW direction and borders in the south on the Izu-Bonin Trench. In the north, the JT intersects with the Kuril Trench at the Erimo Seamount (Fig. 1). The incoming Pacific plate is characterized by NNE-SSW trending horst-graben structures linked to extension on the downward bending subducting plate, resulting in rough topography with typical graben-fill and trench-fill basins

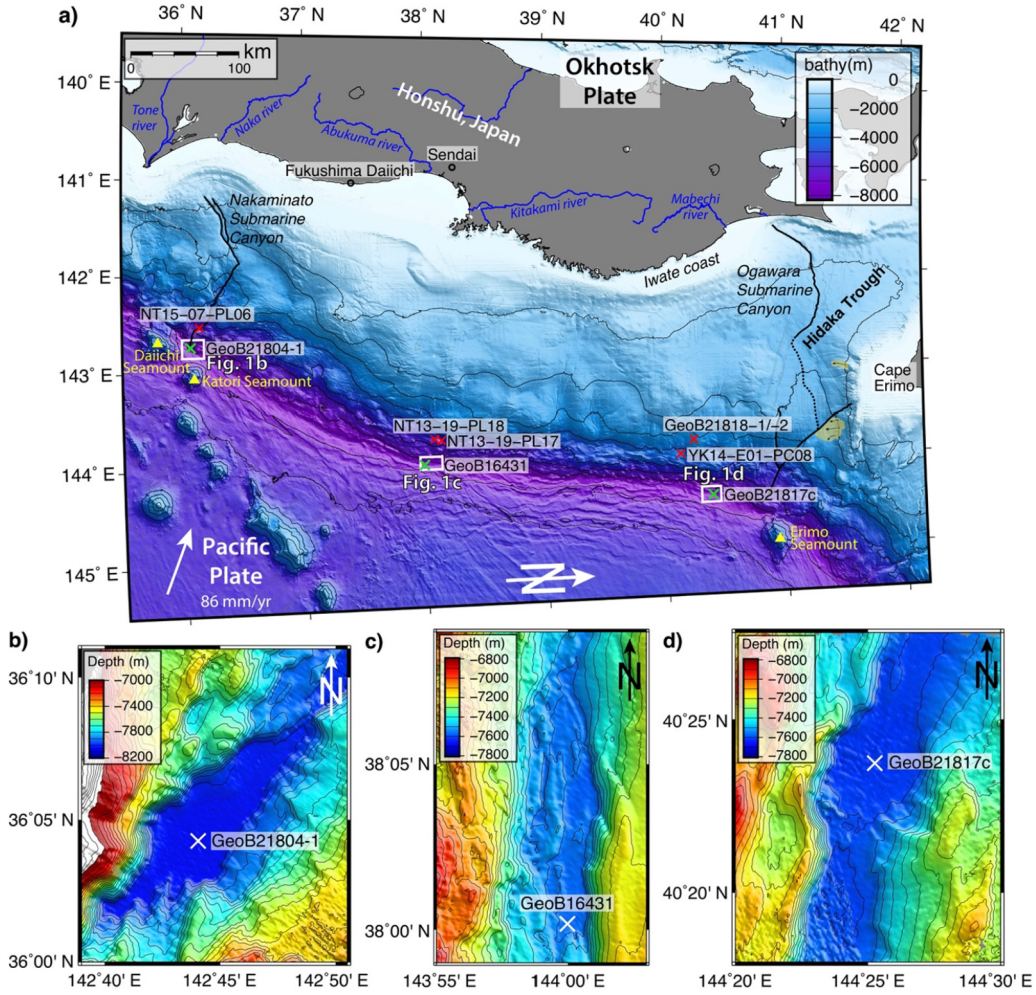

Fig. 1. a) Bathymetric overview map of the Japan Trench (Strasser et al., 2017; Kioka et al., 2019a) between the Daiichi Seamount in the South and the Erimo Seamount in the North with 1000-m contour lines. Red crosses mark core locations on the slope, whereas green crosses mark core locations in the trench. Black bold lines mark the Nakaminato and Ogawara canyon in the South and North, respectively. Yellow shaded areas off Cape Erimo indicate scarps of submarine landslides of unknown age. (note clockwise-rotation of the map by 90 degrees) b) Bathymetric map of the southern basin with 50-m contour lines and core location GeoB21804-1; c) Bathymetric map of the central basin with 50-m contour lines and core location GeoB16431; d) Bathymetric map of the northern basin with 50-m contour lines and core location GeoB21817c. (For interpretation of the colors in the figure(s), the reader is referred to the web version of this article.)

(Kioka et al., 2019a). Water depths of trench basins are ~7,400 m in the north (Fig. 1b), 7,600 m in the central basin (Fig. 1c), and 8,030 m in the southern basin, north of Daiichi-Kashima seamount (Fig. 1d) (Kioka et al., 2019a). The landward slope is divided into a gently dipping upper slope with occurrence of isolated basins (e.g., Arai et al., 2014), and a more steeply dipping lower slope with ~5° (Kawamura et al., 2012). The lower slope is characterized by trench-parallel lineaments, which are related to reverse and normal faults (Tsuji et al., 2011). The existence of a mid-slope terrace, extending from the central JT (~5,500 m) to the northern JT (~4,000 m), might relate to the development of an accretionary prism (e.g., Tsuji et al., 2011).

On eastern Honshu, major river systems, such as the Tone and Naka rivers (SE), the Abukuma and Kitakami rivers (E), and the Mabechi river (NE) (Fig. 1) have the capability to transport terrestrial carbon from their respective watersheds to the ocean. Two canyon systems – the Ogawara canyon in the north and the Nakaminato in the south – connect the shelf area with the trench (Fig. 1). These canyons are classified as Type II shelf-incising canyons (Harris and Whiteway, 2011) and potentially facilitate transfer of terrestrial OC to the hadal realm. Several small channel structures confined to the lower and upper slope (i.e., Type III canyons; Harris and Whiteway, 2011) occur between these two Type II canyons (e.g., Kawamura et al., 2012). Calculated flow accumulations within the JT (Kioka et al., 2019b) indicate that the central basin (Fig. 1c) is not affected by a canyon system.

Sediment along the trench and lower slope consists mainly of diatom frustules and diatomaceous mud due to high regional marine primary production supported by upwelling of nutrient-rich waters resulting from the mixing of the warm Kuroshio and Tsugaru current with the cold Oyashio current (Ikehara et al., 2016). On the upper slope, above the carbonate compensation depth (CCD ~4,500 m, Berger et al., 1976), calcareous and diatomaceous mud with clastic and volcanic grains were found (e.g., Arita and Kinoshita, 1984; Strasser et al., 2017). Sediment in the Nakaminato Canyon consists mainly of clayey-silt frequently interbedded with sand layers and sand patches, based on cores NT15-07-PL06 and PC06 (JAMSTEC, 2015).

The sedimentary succession in the entire JT is heavily affected by event deposits (e.g., turbidites). These deposits have been mapped and correlated along the trench using hydro-acoustic sub-bottom profiles and sediment cores (Ikehara et al., 2016; Kioka et al., 2019b). Several of the event layers have been dated by means of tephrochronology and radiocarbon of bulk OC and correlated to major historic earthquakes, such as the 2011 Tohoku-oki earthquake, the AD1677 Empo-Boso-oki earthquake, AD 1454

Kyotoku earthquake, the AD 869 Jogan earthquake, and an older earthquake in the 2nd to 3rd century BP (Ikehara et al., 2016; Kioka et al., 2019b). One event, however, potentially correlates to the AD 1856 Edo-Ansei typhoon (Kioka et al., 2019b).

Event deposits triggered by the 2011 Tohoku-oki earthquake contain high excess ^{210}Pb (Ikehara et al., 2016; Kioka et al., 2019a; McHugh et al., 2016, 2020) and were described as products of surficial sediment remobilization (Kioka et al., 2019a; McHugh et al., 2016, 2020). This earthquake-shaking induced process remobilizes over wide areas only a few cm of organic-rich surface sediment (e.g., Molenaar et al., 2019), which is then mobilized downslope as dilute fine-grained turbidity currents into deeper basins. This remobilization process can transfer relatively large amounts of carbon to the hadal trench (Kioka et al., 2019a).

3. Methods

3.1. Sampling material and strategy

We primarily analyzed piston core GeoB21804-1 (36.07093°N/142.73408°E, 8025 m water depth) from the southern Japan Trench (JT), composite core GeoB21817c established from cores GeoB21817-1/-2 (supplementary text S1 and figure S1; 40.39558°N/144.42093°E, 7607 m water depth) from the northern JT and two samples from core GeoB21818-1/-2 (40.24648°N/143.81345°E, 3138 m water depth), retrieved on the northern slope (Fig. 1a). All three cores were collected during R/V *Sonne* cruise SO251a in 2016 (Strasser et al., 2017). Cores were opened and described onboard and were shipped to MARUM–Center for Marine Environmental Sciences, where they were stored at 4 °C and subsequently sampled. Samples used for further analysis were stored at −20 °C at ETH Zürich.

Altogether, 24 samples from GeoB21804-1 (south), 8 samples from GeoB21817c (north) and 2 samples from GeoB21818-1/-2 were analyzed. The majority of these samples were collected within event deposits, to analyze bulk OC signatures. Sample preparation and measurements were following the procedures after Bao et al. (2018b) and Kioka et al. (2019b) (see details in sections 3.2, 3.4, 3.5), in order to facilitate comparison of prior results with newly acquired data from this study.

To investigate the margin-wide bulk OC ^{14}C age offset at the surface, surface sediment (0-1 cm) of 5 slope cores (Supplementary table S1) collected during Japanese and German research cruises, have been sampled and analyzed. For trench cores, samples were chosen from thin oxidized layer right below the base of the 2011 Tohoku-oki earthquake event deposit TT1 representing the 2011 paleosurface (Ikehara et al., 2016), since bulk OC of current surface samples (0-1 cm) might be biased by the mixed carbon within the event deposit.

Molar TOC/TN ratios (hereafter: TOC/TN) were measured on all bulk OC ^{14}C samples (also the ones presented by Kioka et al. (2019b) and Usami et al. (2021)). Stable carbon isotope compositions (δ^{13}C) of bulk OC were determined on 20 samples corresponding to hemipelagic background sedimentation and event deposits of cores GeoB21804-1 and GeoB21817c. Results were compared with data from the central basin (Bao et al., 2018b) to further examine the sediment and carbon flux through the canyons.

Fifteen selected samples of GeoB21804-1, GeoB21817c, and GeoB21818-1/-2 were subject to RPO to derive information on the compositional and age heterogeneity within bulk organic matter. Samples were selected to enable comparison between hemipelagic background sediment and individual event deposits. Sample preparation and measurements followed procedures after Bao et al. (2018b; details in the following sections) to compare the results from the central JT (Bao et al., 2018b) with our findings from the northern and southern JT and slope.

3.2. Sample preparation 1: HCl fumigation

Samples for bulk OC ^{14}C, TOC/TN, and bulk OC δ^{13}C analyses were freeze-dried and powdered. 10-35 mg (analysis dependent) of the powdered samples were weighted into pre-combusted Ag capsules, placed on a ceramic tray in a desiccator, and fumigated for 72 h at 60 °C with ∼30 ml of concentrated HCl (37%, metal-trace purity). Afterwards, the acidified samples were neutralized with ∼20 g NaOH pellets for another 72h at 60 °C.

3.3. Sample preparation 2: HCl rinsing

Due to instrumental constraints at the time of δ^{13}C analyses (see supplementary information Text S2), an additional set of 10 samples of core GeoB21804-1 were analyzed for bulk OC δ^{13}C to investigate influence of the canyon. For this, ∼10 mg of powdered samples were filled into 15-ml centrifugal tubes and filled with ∼3 ml of 6 molar HCl. The reaction was left for ∼12 hours. Acidified samples were centrifuged for 4 minutes with 3000 rotations/min to separate the supernatant liquid from the solid material. Samples were neutralized with deionized water and centrifuged for 5 min with 3000 rotations/min for at least 3 times, before they were dried for three days in an oven at 50 °C. Once dry, samples were ground with an agate mortar and filled into small valves.

3.4. Bulk OC analysis

Fumigated samples were analyzed for TOC, TN, bulk OC ^{14}C on the coupled elemental analyzer EA-IRMS-AMS online system at ETH Zürich (McIntyre et al., 2017). The 15 fumigated bulk sediment samples, processed on the RPO (section 3.5), were analyzed for bulk OC δ^{13}C utilizing an elemental analyzer coupled to Precision-Isoprime. Ten samples rinsed with HCl were analyzed for bulk OC δ^{13}C by means of an elemental analyzer (Thermo-Fisher-Delta-V with Flash EA) of the Climate Geology group at ETH Zürich. (See supplementary information Text S2 for detailed calibration of all measurements). All ^{14}C results are reported as uncalibrated ^{14}C bulk ages throughout the manuscript.

3.5. Ramped pyrolysis/oxidation (RPO)

In addition to bulk-level measurements, 15 bulk sediment samples were subjected to ramped temperature pyrolysis/oxidation (RPO, Rosenheim et al., 2008) at the National Ocean Science Accelerated Mass Spectrometer facility (NOSAMS) at Woods Hole Oceanographic Institution (WHOI). For these analyses, 100-150 mg of acid-fumigated samples (as described in section 3.2) were loaded into a quartz reactor and were heated and oxidized at a constant temperature increase of 5 °C min^{-1} to ∼990 °C (Bao et al., 2018b; Rosenheim et al., 2008). The resulting gas was transported out of the reactor by using a He-O_2-carrier gas (∼8% O_2, total flowrate 35 mL/min, oxidation mode) and passed under isothermal condition a catalyst wire (∼800 °C), a chemical trap (∼450 °C; containing CuO, Ag, and MnO granules) and a water trap (−86 °C) in order to purify the gas, to bind other combustion gases as Cl_2 and SO_2, and to remove H_2O, respectively. After passing a flow-through infrared CO_2 analyzer (Sable-Systems-International-Inc., CA-10a) to measure the CO_2 concentration, the purified CO_2 of 5 temperature intervals (T_1: 170-320 °C; T_2: 320-391 °C; T_3: 391-486 °C; T_4: 486-570 °C; and T_5: 570-915 °C; after Bao et al., 2018b) was sequentially isolated and trapped into pre-combusted glass tubes. At the beginning of each experiment and once within every temperature interval, leak checks were conducted. The purified CO_2 was measured as gas at the ETH AMS facility.

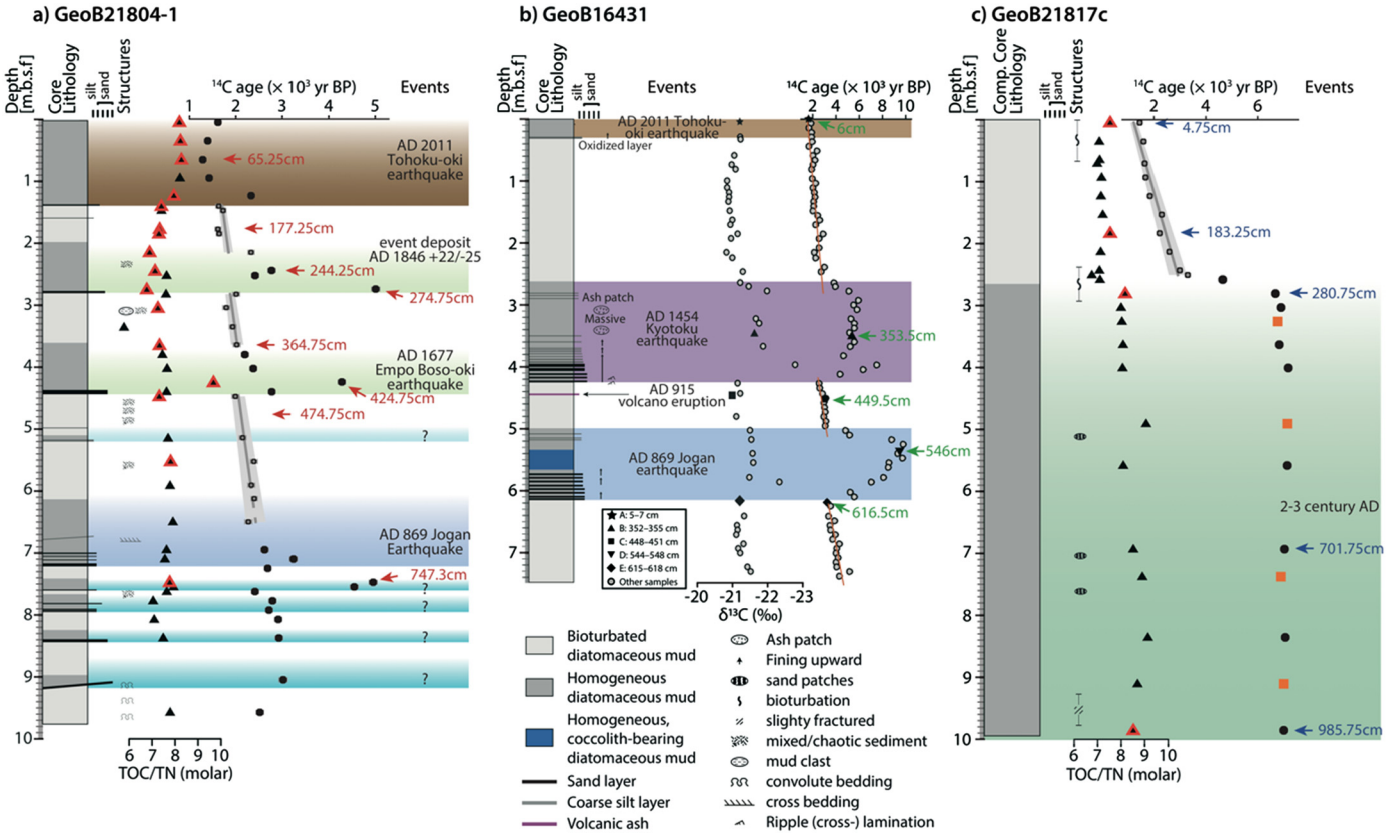

Fig. 2. a) Core GeoB21804-1 collected in the southern basin with litholog (after Strasser et al., 2017), TOC/TN (triangles), bulk OC ^{14}C ages (circles), and interpretation of event deposits (after Kioka et al., 2019b). b) Reference core Geob16431 from the central basin with litholog (Ikehara et al., 2016), bulk OC δ^{13}C values and bulk OC ^{14}C ages (data of Bao et al. (2018b)). c) Core GeoB21817c retrieved in the northern basin with litholog (after Strasser et al., 2017), TOC/TN, and bulk OC ^{14}C ages. Triangles with red border in a) and c) were further analyzed for δ^{13}C. Bulk OC ^{14}C ages within the background sediment in a) and c) are after Kioka et al. (2019b). Four bulk OC ^{14}C ages marked with orange rectangles are after Usami et al. (2021). Samples marked with red (a), green (b), and blue (c) arrows were further processed on the RPO (samples in (b) by Bao et al., 2018b).

Resulting data from RPO was further subject to a regularized inverse method to estimate the distribution of OC activation energy, which is a proxy for molecular bond strength and chemical structure of the OC (Hemingway et al., 2017). The distribution of the OC activation energy was calculated by using the default setting of the open source Python package "rampedpyrox" (Hemingway, 2018).

4. Results

4.1. Bulk OC analysis

4.1.1. GeoB21804-1 (south)

Bulk OC ^{14}C measurements reveal a wide spectrum of ages, ranging from 1288±60 to 5009±90 yr BP (Fig. 2a). In the upper part of the core (<720.0 cm), where a linear relationship between inter-event-deposit background sediment and bulk OC ^{14}C ages has been documented by Kioka et al. (2019b), our new age data represent mainly older bulk ages of the event deposits. Thick event deposits are absent from the lower part (>720.0 cm) of the core, and instead this interval contains only thin deposits resulting from minor sediment remobilization processes. For this section, most of our new bulk OC ^{14}C data define the downward projected linear age increase trend of background sediment, with only two samples indicating old ages within a small sediment remobilization deposit (red arrow 747.3 cm in Fig. 2a). The sandy bases of event deposits show generally the oldest ages (e.g., 5009±90 yr BP at 274.75 cm) whereas the overlying homogeneous diatomaceous mud usually have younger ages. TOC/TN reveals values from 5.78-9.67 (mean=7.59, standard deviation(sd)=0.59, n=35), and TOC content from 0.54%-2.41% (mean=1.42% sd=0.45%, n=35; Fig. 2a, supporting information table S2). The δ^{13}C measurements (fumigated) range between −21.22 ‰ and −20.10 ‰ (mean=−20.75 ‰, sd=0.38 ‰, n=8) and the rinsed samples between −21.85 ‰ and −21.47 ‰ (mean=−21.65 ‰, sd=0.13 ‰, n=10; supporting information table S2).

4.1.2. GeoB21817c (north)

Bulk OC ^{14}C ages of core GeoB21817c range from 4648±78 yr BP at the transition of hemipelagic background sediment to event deposit to 7173±91 yr BP within the event deposit (Fig. 2c). These ages correspond to the upper 7 m of an approximately 10 m thick event deposit (Kioka et al., 2019b). The 8 samples collected within the event deposit show very constant ages that vary between 6679±87 and 7173±91 yr BP (mean=6975 yr BP). TOC/TN range between 6.76 and 9.14 (mean=7.79, sd=0.72, n=24), TOC content between 0.9% and 1.55% (mean=1.27%, sd=0.13%, n=24; Fig. 2c), and δ^{13}C of fumigated samples between −21.96 ‰ and −19.83 ‰ (mean=−20.95 ‰ sd=0.76 ‰, n=4; supporting information table S3).

4.1.3. Surface sediment samples

In order to assess age offsets at the sediment surface, core-top (0-1 cm) samples were analyzed from the slope cores. Core GeoB21817c in the northern basin was sampled at a depth interval of 4 to 5.5 cm, whereas cores GeoB21823 (same core location as GeoB16431) and GeoB21804-1 from the central and southern basin, respectively, were sampled below the base of the AD 2011 event deposit, representing the sediment surface at 2011. The sam-

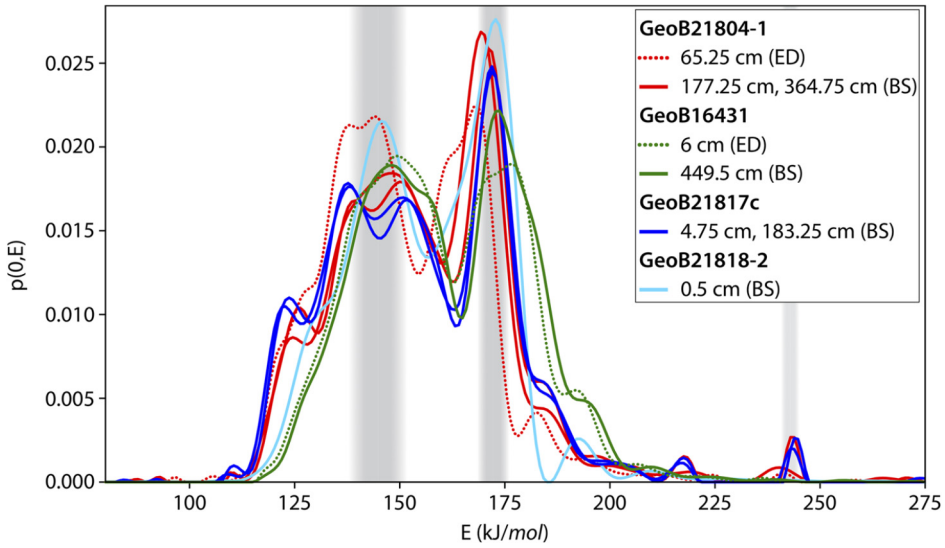

Fig. 3. Activation energy distributions of background sediments (BS) from the four different core locations GeoB21804-1 southern Japan Trench (red), GeoB16431 central Japan Trench (green), GeoB21817c northern Japan Trench (blue), GeoB21818-2 northern slope (cyan) in solid lines, and of event deposits of the 2011 Tohoku-oki earthquake from the southern Trench (red dotted line) and the central Japan Trench (green dotted line). The three vertical, gray bars illustrate the range of the two primary peaks between ~138 and 152 kJ/mol and ~167 and 174 kJ/mol) and the secondary peak between (240-245 kJ/mol).

ples yield bulk OC ^{14}C ages varying between 1431±75 yr BP and 1796±75 yr BP with an average of 1581±74 yr BP (supporting information table S1). We note that the oldest age (1796±75 yr BP) is from a surface sample from the Nakaminato canyon. Nevertheless, the data indicate a consistently smaller age offset at the northern study site (1451±74 yr BP) than at the central and southern study sites (1623±78 yr BP and 1714±69 yr BP, respectively). TOC/TN range between 7.02 and 8.24 (mean=7.55, sd=0.43, n=8), TOC between 0.80% and 1.74% (mean=1.50%, sd=0.29%, n=8). δ^{13}C was measured on 3 samples and range between −21.85 ‰ and −20.70 ‰.

4.2. Ramped pyrolysis/oxidation

Fifteen samples from different sedimentation phases (i.e., hemipelagic background sediment and event deposits) and different core locations (i.e., northern and southern JT and northern slope) were subject to RPO. Thermograms generally indicate two peaks at temperatures of 316-341 °C (peak 1) and 411-443 °C (peak 2), respectively (Supporting information Figure S2). In some samples (e.g., GeoB21804-1 177.25 cm, GeoB21817c 4.75 cm), a third small peak can be observed at about 737-745 °C. ^{14}C measurements of evolved carbon fractions corresponding to the individual temperature intervals (T_1-T_5) from the 15 samples exhibit overall increasing ^{14}C ages with increasing temperature (i.e., from T_1 to T_5; supporting information Figure S2). Sample GeoB21818-1 6.75 cm represents the only exception, where T_3 shows the oldest ^{14}C age and T_5 youngest.

Apparent activation energies calculated from thermograms indicate a wide distribution from ~100 kJ/mol to ~300 kJ/mol with similar peaks among samples (supporting information figure S3). The results reveal striking similar peak distributions for background sediment in the north (GeoB21817 4.75 cm, 183.25 cm) and in the south (GeoB21804 177.25 cm) of the trench (Fig. 3). Event deposits differ only partly in activation energy peak distribution. The primary peaks between ~167 and 174 kJ/mol and between ~138 and 152 kJ/mol are evident in all samples (Fig. 3, and supporting information Figure S3). Smaller, secondary peaks cannot be constantly traced through all samples.

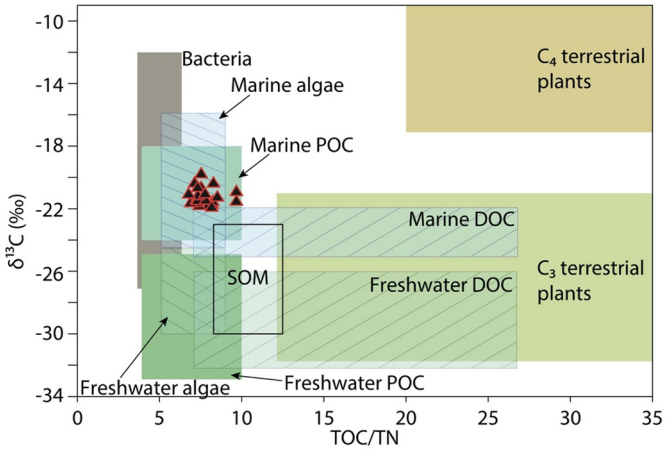

Fig. 4. Diagram (modified after Goni et al., 2008 and Lamb et al., 2006, and references therein) indicating the provenance of the samples based on TOC/TN and δ^{13}C, indicating marine origin (POC = particulate organic carbon, SOM = soil organic matter, DOC = dissolved organic matter). Triangles indicate Japan Trench sediments.

5. Discussion

5.1. Trench-wide constraints on the nature and provenance of OC

Marine organic matter (MOM) generally consists of abundant nitrogen-rich compounds (e.g., proteins), whereas terrestrial organic matter contains carbon-rich structural polymers (e.g., cellulose, lignin, cutin and cutan (e.g., Hedges et al., 1997). These biochemical variations, together with different carbon isotopic fractionation characteristics, can result in distinct TOC/TN and isotopic compositions (δ^{13}C values) of marine and terrestrial organic matter (Fig. 4). TOC/TN and δ^{13}C are thus widely used to determine the provenance of organic matter (e.g., Goni et al., 2008; Lamb et al., 2006). TOC/TN of MOM typically varies between 5.78 and 9.67 and δ^{13}C values between −19 ‰ and −22 ‰, whereas TOC/TN of terrestrial organic matter (C3-plants) are ≥20 and δ^{13}C values range between −25 ‰ and −28 ‰ (e.g., Goni et al., 2008; Hedges et al., 1997). δ^{13}C values for C4 ecosystems would be significantly less negative.

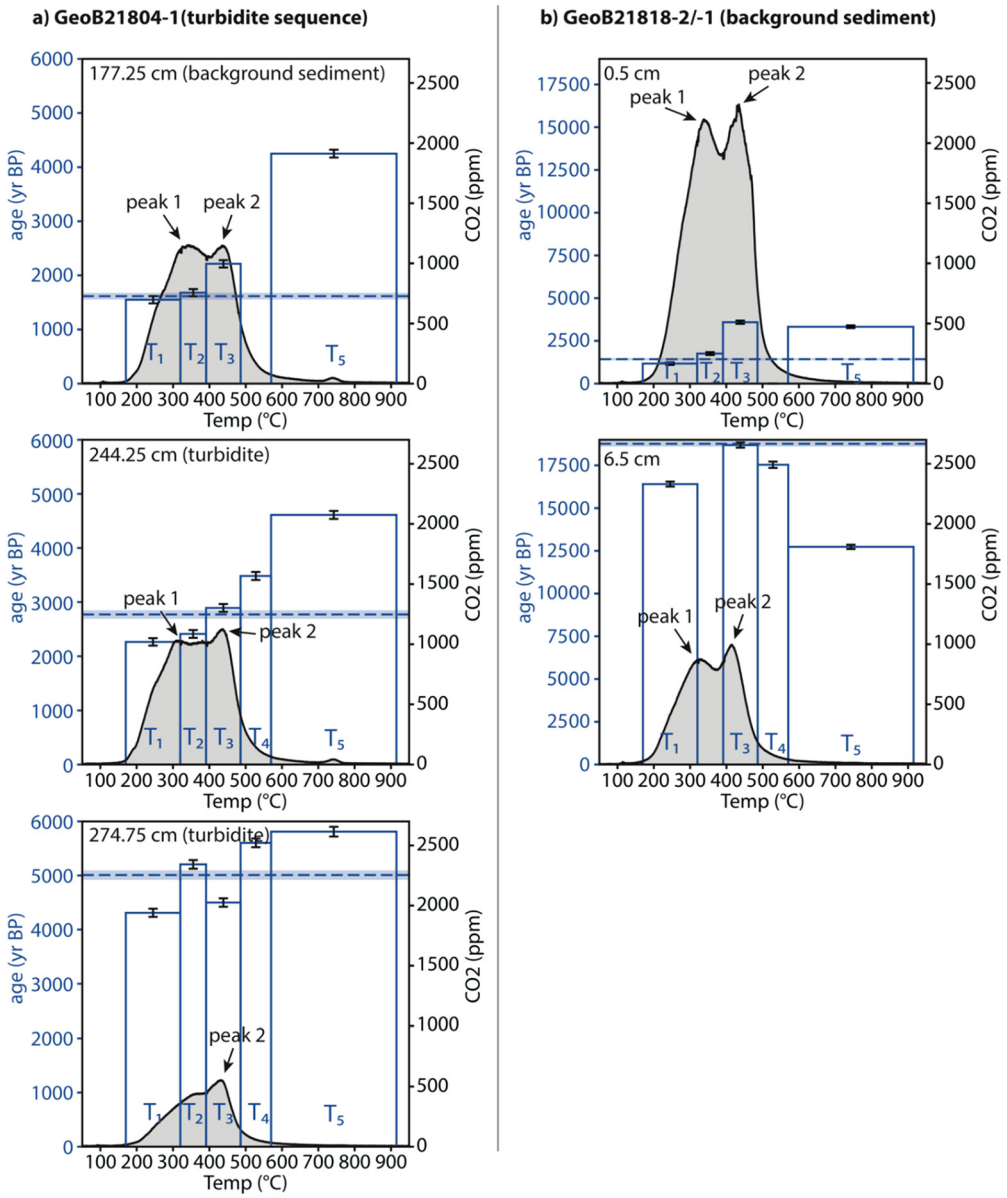

Fig. 5. a) Sequence from background sediment (177.25 cm) to turbidite (244.75 cm and 274.75 cm) of core GeoB21804-1 present an age increase in all 5 temperature fractions (T_1–T_5), indicating remobilization of slightly older carbon. The thermograms show an overall decrease in TOC content towards the base of the turbidite, especially of peak 1, which disappears in sample 274.75 cm. b) Thermograms of hemipelagic background sediments of the slope core GeoB21818-2/-1 present decreased TOC content within older sediment, while peak 1 and 2 remain similar.

TOC/TN of the analyzed Japan Trench (JT) samples vary between 6 and 10 and bulk OC $\delta^{13}C$ range between −19.83 ‰ and −21.96 ‰, suggesting that the bulk OC mainly consists of MOM (marine particulate organic carbon (POC), and marine algae; Fig. 4). Given the geographic location and the low TOC/TN values significant C4 contribution can be excluded. Our observation that sediment in the JT mainly contains MOM, in particular marine algae is thus in line with previous studies based on molecular analyses and stable isotopes (Ishiwatari et al., 2000) and the bulk OC $\delta^{13}C$ data (Bao et al., 2018b).

Further, activation energy distributions (inversely modeled from thermal decay of OC) of background sediment from the southern, central and northern JT show strikingly similar profiles (Fig. 3 and supplementary figure S3). Also, within turbidites, the primary peaks in the activation energy distribution mirror those of hemipelagic background sediment (Fig. 5a). Peaks below ∼160 kJ/mol, representing mainly temperature fractions T_1 and T_2 within the first peak of the thermogram at ∼316-341 °C, lie in the range of thermal decomposition of biopolymers (e.g., proteins and carbohydrates) of marine algae and marine POC (e.g., Sanchez-Silva et al., 2012). The activation energy peak between ∼165 and 180 kJ/mol, representing thermogram peak ∼411-443 °C and mainly temperature fraction T_3, is attributed to aggregated and/or encapsulated POC (Bao et al., 2018a, 2019) as well as carbon held within mineral pores (Hemingway et al., 2019), where slightly more energy is necessary for thermal decomposition. The small peaks at 240-245 kJ/mol are expected to correspond to the third small peak in the thermogram at 737-745 °C. This high temperature peak lies in the range of the thermal decomposition of calcite polymorph (Karunadasa et al., 2019) and is, thus, inferred to stem from remnant IC, which escaped removal via fumigation. Alternatively, the third peak could represent liberation of carbon tightly held within clay minerals during the temperature-stepped combustion (Wang et al., 2016) or could be minor contributions by rock-derived OC (e.g., graphite).

These above analyses suggest that OC deposition over the entire trench-slope system is similar, regardless of the presence or absence of canyons. Moreover, the similarities between hemipelagic background sediment and event deposits in terms of activation energies, TOC/TN and $\delta^{13}C$ reveal OC with similar bonding environment (i.e., a common OM composition and sediment fabric) that is primarily of marine origin. This trench-wide similarity in OC composition potentially reflects the high levels of marine primary production over this region, implying that event deposits originate primarily from adjacent slopes and that the canyons do not transfer significant amounts of terrestrial OC to the trench.

5.2. Trigger mechanism(s) of event-related sediment and carbon transport to the trench

Based on our $\delta^{13}C$ and TOC/TN data, we conclude that, in contrast to e.g., the MT (Kao et al., 2010), hyperpycnal flows associated with flood events (e.g., during typhoons that result in intense discharge of terrestrial organic matter) do not reach the JT. This also is in line with the lack of typhoon-related breaks of submarine telecommunication cables in our study area, which have been recorded elsewhere (e.g., around Taiwan, northern Philippines, and southwestern Japan; Pope et al., 2017). Hence, the event deposit dated by Kioka et al. (2019b) to AD 1846 +22/-25 might not be related to the AD 1856 Edo-Ansei Typhoon, according to our new result. Nevertheless, our investigation, as well as other studies in high-seismicity areas (e.g., Hikurangi Trough; Mountjoy et al., 2018) show that earthquakes are key events leading to transfer of large amounts of sediment and carbon to the deep sea. Since the event deposits and hemipelagic background sediments exhibit similar bulk OC signals (i.e., TOC/TN or $\delta^{13}C$), we infer that all analyzed event deposits – including the ~AD 1846 event (Kioka et al., 2019b) – are earthquake-triggered, and that they originate from the trench slope. These findings corroborate previous interpretations based on event-deposit correlation with historical earthquakes and tsunamis (Ikehara et al., 2016; Kioka et al., 2019b) as well as sediment provenance data by Schwestermann et al. (2020); McHugh et al. (2020) indicating earthquake-triggered surficial slope sediment remobilization.

There may be several reasons for minor terrestrial carbon transfer to the JT compared to other trenches (e.g., MT and the NBT). These include the physiography of the canyons and the shelf width and distance between the coast and trench (NBT: ~60 km distance, average slope angle ~8°, Xiao et al., 2020; JT: >180 km distance, average slope angle <2.5°). The canyons in our study area are neither well developed, nor directly associated with rivers (Harris and Whiteway, 2011). Moreover, the head of the Nakaminato Canyon is over 40 km from the coast and, at a water depth of >400 m, does not incise the shelf, falling under the classification of type III canyon (Harris and Whiteway, 2011). In the north, one branch of the Ogawara Canyon incises the shelf of north eastern Honshu. However, this canyon branch is interrupted by the Hidaka Trough, where turbidity currents might lose the energy and thus the ability to inject sediment and terrestrial carbon into the JT. A second branch of the Ogawara Canyon connects to the south coast of Hokkaido (Cape Erimo, Fig. 1) and intersects the Hidaka Trough at its eastern end. While this branch may support direct sediment and carbon transfer to the JT, it barely incises the shelf, with the canyon head located at the shelf edge more than 40 km from the coast at a water depth of ~200 m.

5.3. ^{14}C constraints on the source and delivery of OC to the hadal trench

Our new bulk OC ^{14}C measurements on event deposits in the southern (core GeoB21804-1) and northern (core GeoB21817) basin indicate overall older ages ($\lesssim$3 kyr and $\lesssim$4 kyr, respectively) compared to the respective both overlying and underlying hemipelagic background sediment dated by Kioka et al. (2019b). Such age discrepancies have previously been found in the central JT (~3 kyr and <6 kyr for the Kyotoku- and Jogan Earthquake event deposits, respectively; Bao et al., 2018b), and indicate remobilization of pre-aged OC (Schwestermann et al., 2020).

Bulk OC ^{14}C ages of core GeoB21804-1 (south) shows four big event deposits (marked in color, after Kioka et al., 2019b) and up to five smaller event deposits (Fig. 2). However, the fine-grained tops of the latter events are barely distinguishable from the background sediment. We therefore focus mainly on the four large event deposits. The first and most recent of these (from top to bottom), which corresponds to the 2011 Tohoku-oki earthquake (Kioka et al., 2019a), reveals the same bulk OC ^{14}C age as that of the underlying sediment, with the exception of the very base of this unit that exhibits an ~0.4 kyr age shift. This observation indicates that freshly deposited sediment including young OC was remobilized, consistent with prior studies that found high excess ^{210}Pb in this event deposit (Kioka et al., 2019a). In contrast, earlier (stratigraphically lower) event deposits exhibit larger ^{14}C age-shifts (max. 3 ka), although the sand bases of these layers typically show substantial age offsets of >1 kyr, whereas age offsets are generally less than 0.5 kyr for the overlying homogeneous diatomaceous mud.

^{14}C ages measured on CO_2 for the five individual temperature fractions (T_1-T_5) from RPO exhibit similar shifts between samples. For example, in turbidite samples exhibiting a shift in bulk OC ^{14}C ages of 1 kyr, each corresponding temperature fraction is also increased by ~1 kyr (Fig. 5). While such age shifts in bulk OC could be explained by preferential degradation of organic matter (e.g., Bao et al., 2019), this explanation is difficult to reconcile with concurrent shifts for all five temperature fractions. Alternatively, age discrepancies, particularly for coarser sediments at the base of turbidites, might result from hydraulic sorting. RPO thermograms show that peak 1 (316-341 °C) decreases in the coarser bases of turbidites compared to peak 2 (411-443 °C) (Fig. 5a, from 177.25-274.75 cm). This asymmetric decrease further supports the interpretation of peak 1 to reflect contributions from relatively labile, low-density POC derived from marine productivity (see 5.1 above) that remains longer in suspension relative to coarser and denser particles (e.g., sand and coarse silt) already deposited (Fig. 5a). This is also supported by the grain-size distributions and TOC content (supporting information Fig. S4, table S2). Peak 2 (411-443 °C), in turn, is interpreted as more recalcitrant OC, or OC protected through close association with mineral grains, or encapsulation within organo-mineral aggregates (e.g., Bao et al., 2018a; Hemingway et al., 2019, section 5.1). This could explain its persistence in the sandy base, as well as the generally older ^{14}C ages of T_3-T_5. This hypothesis is also corroborated by two thermograms of hemipelagic background sediment with comparable OC composition from the northern slope (Fig. 5b) which show a more uniform decrease in TOC content with ^{14}C ages of up to ~15,000 years. Also, homogenous diatomaceous mud of the thick event deposit in the north (GeoB21817c, supporting information Fig. S3) clearly show a higher contribution of peak 1 than evident in the coarser base of the turbidite unit in the south (GeoB21804-1 274.75 cm).

While coarser grain-size can thus partly explain the larger age shifts in bases of turbidites (e.g., GeoB21804-1 274 cm), it cannot explain the smaller age discrepancies in the fine-grained upper part of turbidites. The incorporation of slightly older carbon, such as via deeper erosion of sandy turbidity currents might thus be a third explanation. Following the interpretations of Schwestermann et al. (2020) for the central JT, small age shifts documented for the event deposits of historic earthquakes may reflect remobilization

of surficial slope sediments, from which sandy turbidity currents can evolve that erode into deeper strata.

Core GeoB21817c (north) comprises a single, massive (~10 m thick) event deposit with bulk OC ^{14}C ages that are ~4 kyr older than the overlaying background sediment (Kioka et al., 2019b). This age offset is near constant over the entire 7 meters of the event deposit, indicating very well mixed, homogenous sediment. The base of the turbidite has not been cored, however a sand base can be expected based on the acoustic reflections (Kioka et al., 2019b). Based on observations from event deposits in the southern and central JT, we would expect the sand base to exhibit a larger offset in bulk OC ^{14}C ages. This thick event deposit might relate to a canyon flushing event similar to that observed at the Hikurangi Margin (Mountjoy et al., 2018), and likely originates from submarine landslides on the upper slope (Usami et al., 2021). From geomorphic analyses of the bathymetry map (Fig. 1), we interpret two potential landslide-scars off Cape Erimo (supplementary data figure S5) as a putative source for such a canyon flushing event. However, the age of these two landslides is unknown. Alternatively, large-scale (over broad areas) remobilization of surface sediments, as observed on the northern trench slope (Ikehara et al., 2020; Molenaar et al., 2019), evolving into sandy and erosive turbidity currents in the Ogawara canyon, could be a second explanation. In either case, the constant bulk age of ~7 kyr of the event deposit found in four small trench basins (Usami et al., 2021), as well as the uniform bulk OC ^{14}C age distribution over the 5 temperature fractions (T_1-T_5, this study, supporting information figure S3) points toward a very well-mixed, homogenous event deposit.

5.4. Refined dating and correlation of event deposits in the Japan Trench

The bulk OC ^{14}C ages of surface sediment samples collected in the trench and on the trench slope reveal a decreasing age offset from southern to the northern sections of the study area (1715±70 yr BP in the south, 1623±78 yr BP in the central and 1451±74 yr BP in the north, section 4.1.3, supplementary table S1). Within the same section of the study area, trench slope and trench sediments indicate generally similar ages (except in the south). The large age offset in the south is strongly influenced by the surface sample of core NT15-07-PL06 retrieved within the Nakaminato Canyon. This sample may not be representative, however, due to older sediment and carbon trapped within the canyon. When just considering the age offset from the surface sample in the southern trench (1633±64 yr) it is very similar to the one in the central study area. In contrast, surface sediments in the northern study area have smaller (~175 ^{14}C years) bulk OC age offsets. We attribute this spatial variability to differences in oceanographic setting with higher primary productivity along the Hokkaido coast resulting in relatively enhanced delivery of younger OC to the northern JT (Usami et al., 2021) compared to older, preaged OC. The generally similar surface age offset between trench slope and trench sediments explains that event deposits derived from surficial sediment remobilization (e.g., the 2011 Tohoku-oki earthquake event deposits), have the very similar age offset as the direct under- and overlaying hemipelagic background sediment.

If we apply the newly constrained mean age-offset for the southern trench site (1633 bulk ^{14}C yr, instead of ~1600 bulk ^{14}C yr as used by Kioka et al. (2019b)), the previously published event age for the deposit (AD 1846 (+22/-25)) for which an earthquake vs. typhoon trigger could not be resolved (Kioka et al., 2019b) is now refined to be approximately 33 bulk ^{14}C years younger. Being aware of the uncertainties, this slightly younger "floating" bulk ^{14}C age range better aligns with either the historically documented AD 1896 January M7.3 Ibaraki-oki, or the AD 1897 August M7.7 Sanriku-oki earthquakes than with the earlier AD 1856 Edo-Ansei Typhoon. An earthquake rather than a typhoon trigger is corroborated by the marine carbon provenance of OC in this event deposit (sections 5.1 and 5.2). Applying corrected mean age offsets in the northern study area (i.e., 149 years younger than estimated by Kioka et al. (2019b)), the refined age of the thick event deposit is 1.77 (+0.49/-0.31) bulk OC ^{14}C kyr BP, potentially coeval with tsunami deposits along the Iwate coast (see Fig. 1 for locations) that suggest large earthquake in this area during the 2nd or 3rd Century AD (Takada et al., 2016).

6. Conclusion

This investigation is, to the best of our knowledge, the first to systematically characterize OC signatures in sediments that have been deposited along the axis of an entire hadal oceanic trench system (Japan Trench (JT)) over the past 2 millennia. These new data permit examination of links between event-related carbon transfer to hadal trenches and margin geomorphology as well as potential trigger mechanisms with different rates of recurrence (i.e., lower frequency subduction zone earthquakes vs. higher frequency tropical cyclones). New ^{14}C data emanating from this study also serve to refine dates of prior earthquake-related event deposits in the JT.

Bulk OC ^{14}C age differences between hemipelagic background sediment and event deposits range from ≤3 kyr in the southern JT, <6 kyr in the central JT, to ≤4 kyr in the northern JT. These age offsets, which are usually largest in the lower, sandy layers of event deposits, cannot be solely explained by hydraulic particle sorting or selective preservation of OC. For the southern and central JT, we attribute the offsets to earthquake-triggered remobilization of surficial sediments (including tephra layers) that evolve into erosive turbidity currents entraining older carbon. For the northern JT, sporadic canyon flushing events (potentially initiated by submarine landslides in upslope Hidaka Trough) result in remobilization and translocation of vast amounts of sediment and OC to the hadal zone.

Deposition of marine OC predominates along the entire JT system, including within event deposits. This suggests (*i*) that canyon systems do not efficiently funnel terrestrial OC to the hadal zone and (*ii*) that typhoons do not serve as important triggers for sediment and carbon transfer to the JT. These findings lend support to prior observations from the JT indicating that event deposits originated from the landward trench slope and were triggered by earthquake shaking. These findings contrast with those from other trenches (e.g., NBT, MT) where substantial delivery of terrestrial OC to the hadal zone has been observed. These differences can be explained by the large distance between the trench and adjacent landmasses (>180 km), and by the physiography of the canyons feeding the JT. Based on these findings, we suggest that sedimentation processes in hadal trench systems may vary spatially and temporally, and that the source, transfer, and deposition of OC in hadal trenches should not be generalized. High spatial and temporal-resolution sampling of hadal trench sedimentary successions, coupled with advanced carbon isotopic measurements, are necessary for detailed characterization of the mechanics and dynamics of trench systems. Applying such approaches to other trenches and comparing knowledge gained across different hadal environments would contribute towards a holistic understanding of OC transfer, deposition, and burial in trench systems and their role in the carbon cycle and ecology of the deepest ocean realms.

CRediT authorship contribution statement

TS and NH analyzed OC data.

TS and APM conducted ramped pyrolysis/oxidation measurements.

MS, TIE, and TS projected the study.

TS prepared the figures.

TS, MS, and TIE wrote the manuscript with inputs from all authors.

Declaration of competing interest

The authors declare that they have no known competing financial interests or personal relationships that could have appeared to influence the work reported in this paper.

Acknowledgement

We thank captain and crew of the onboard assistance during cruise SONNE 251-1 in 2016. The cruise was supported by the German Bundesministerium für Bildung und Forschung (BMBF 03G0251A) and the Deutsche Forschungsgemeinschaft. We acknowledge the Kochi core repository for additional surface samples of Japanese Cruises. Al Gagnon and Mary Lardie are thanked for their great help and technical assistance with the RPO instrument at NOSAMS. APM and the NOSAMS work were supported by the National Science Foundation Cooperative Agreement OCE-1239667. We appreciate the assistance from members of the Laboratory of Ion Beam Physics for the AMS measurements. Rui Bao is acknowledged for helpful discussions. A special thank you goes to Madalina Jaggi for her technical assistance for the $\delta^{13}C$ analysis of rinsed samples. This study was supported by the Austrian Science Fund (FWF P29678-N28) and a postgraduate grant by the International Association of Sedimentologists (IAS). We also acknowledge constructive support by the two reviewers (Jordon Hemingway and an anonymous). The authors declare no conflict of interests. The bathymetric data used in figure 1 is available at JAMSTEC-DARWIN database (http://www.godac.jamstec.go.jp/darwin/e) and Bundesamt für Seeschifffahrt und Hydrographie (https://www.bsh.de/DE/DATEN/Ozeanographisches_Datenzentrum/Vermessungsdaten/Nordpazifischer_Ozean/nordpazifik_node.html). Data of carbon analyses are displayed in the supporting information and also available from the corresponding author on reasonable request.

Appendix A. Supplementary material

Supplementary material related to this article can be found online at https://doi.org/10.1016/j.epsl.2021.116870.

References

Arai, K., Inoue, T., Ikehara, K., Sasaki, T., 2014. Episodic subsidence and active deformation of the forearc slope along the Japan Trench near the epicenter of the 2011 Tohoku Earthquake. Earth Planet. Sci. Lett. 408, 9–15. https://doi.org/10.1016/j.epsl.2014.09.048.

Arita, M., Kinoshita, Y., 1984. Sedimentological Map of off Kamaishi. Geological Survey of Japan.

Bao, R., McNichol, A.P., McIntyre, C.P., Xu, L., Eglinton, T.I., 2018a. Dimensions of radiocarbon variability within sedimentary organic matter. Radiocarbon 60 (03), 775–790. https://doi.org/10.1017/RDC.2018.22.

Bao, R., Strasser, M., McNichol, A.P., Haghipour, N., McIntyre, C., Wefer, G., Eglinton, T.I., 2018b. Tectonically-triggered sediment and carbon export to the Hadal zone. Nat. Commun. 9 (1), 121. https://doi.org/10.1038/s41467-017-02504-1.

Bao, R., Zhao, M., McNichol, A., Wu, Y., Guo, X., Haghipour, N., Eglinton, T.I., 2019. On the origin of aged sedimentary organic matter along a river-shelf-deep ocean transect. J. Geophys. Res., Biogeosci. 124 (8), 2582–2594. https://doi.org/10.1029/2019JG005107.

Bartlett, D.H., 2009. Microbial life in the trenches. Mar. Technol. Soc. J. 43 (5), 128–131. https://doi.org/10.4031/MTSJ.43.5.5.

Berger, W.H., Adelseck, C.G., Mayer, L.A., 1976. Distribution of carbonate in surface sediments of the Pacific Ocean. J. Geophys. Res. 81 (15), 2617–2627. https://doi.org/10.1029/JC081i015p02617.

DeMets, C., Gordon, R.G., Argus, D.F., 2010. Geologically current plate motions. Geophys. J. Int. 181 (1), 1–80. https://doi.org/10.1111/j.1365-246X.2009.04491.x.

Glud, R.N., Berg, P., Thamdrup, B., Larsen, M., Stewart, H.A., Jamieson, A.J., et al., 2021. Hadal trenches are dynamic hotspots for early diagenesis in the deep sea. Commun. Earth Environ. 2 (1), 21. https://doi.org/10.1038/s43247-020-00087-2.

Glud, R.N., Wenzhöfer, F., Middelboe, M., Oguri, K., Turnewitsch, R., Canfield, D.E., Kitazato, H., 2013. High rates of microbial carbon turnover in sediments in the deepest oceanic trench on Earth. Nat. Geosci. 6 (4), 284–288. https://doi.org/10.1038/ngeo1773.

Goldfinger, C., 2009. Chapter 2B Sub-Aqueous Paleoseismology, 2nd ed. International Geophysics, vol. 95. Elsevier Inc., pp. 119–170.

Goni, M.A., Monacci, N., Gisewhite, R., Crockett, J., Nittrouer, C., Ogston, A., et al., 2008. Terrigenous organic matter in sediments from the Fly River delta-clinoform system (Papua New Guinea). J. Geophys. Res. 113 (F1), F01S10. https://doi.org/10.1029/2006JF000653.

Harris, P.T., Whiteway, T., 2011. Global distribution of large submarine canyons: geomorphic differences between active and passive continental margins. Mar. Geol. 285 (1–4), 69–86. https://doi.org/10.1016/j.margeo.2011.05.008.

Hedges, J.I., Keil, R.G., Benner, R., 1997. What happens to terrestrial organic matter in the ocean? Org. Geochem. 27 (5–6), 195–212. https://doi.org/10.1016/S0146-6380(97)00066-1.

Hemingway, J.D., 2018. rampedpyrox: open-source tools for thermoanalytical data analysis. http://pypi.python.org/pypi/rampedpyrox.

Hemingway, J.D., Rothman, D.H., Grant, K.E., Rosengard, S.Z., Eglinton, T.I., Derry, L.A., Galy, V.V., 2019. Mineral protection regulates long-term global preservation of natural organic carbon. Nature 570 (7760), 228–231. https://doi.org/10.1038/s41586-019-1280-6.

Hemingway, J.D., Rothman, D.H., Rosengard, S.Z., Galy, V.V., 2017. Technical note: an inverse method to relate organic carbon reactivity to isotope composition from serial oxidation. Biogeosciences 14 (22), 5099–5114. https://doi.org/10.5194/bg-14-5099-2017.

Ikehara, K., Kanamatsu, T., Nagahashi, Y., Strasser, M., Fink, H., Usami, K., et al., 2016. Documenting large earthquakes similar to the 2011 Tohoku-oki earthquake from sediments deposited in the Japan Trench over the past 1500 years. Earth Planet. Sci. Lett. 445, 48–56. https://doi.org/10.1016/j.epsl.2016.04.009.

Ikehara, K., Usami, K., Kanamatsu, T., 2020. Repeated occurrence of surface-sediment remobilization along the landward slope of the Japan Trench by great earthquakes. Earth Planets Space 72 (1), 114. https://doi.org/10.1186/s40623-020-01241-y.

Ishiwatari, R., Yamada, K., Matsumoto, K., Naraoka, H., Yamamoto, S., Handa, N., 2000. Source of organic matter in sinking particles in the Japan Trench: molecular composition and carbon isotopic analyses. In: Dynamics and Characterization of Marine Organic Matter. Springer, pp. 141–168.

Jamieson, A.J., Fujii, T., Mayor, D.J., Solan, M., Priede, I.G., 2010. Hadal trenches: the ecology of the deepest places on Earth. Trends Ecol. Evol. 25 (3), 190–197. https://doi.org/10.1016/j.tree.2009.09.009.

JAMSTEC, 2015. NATSUSHIMA "Cruise Report" NT15-07. http://www.godac.jamstec.go.jp/catalog/data/doc_catalog/media/NT15-07_all.pdf.

Jumars, P.A., Hessler, R.R., 1976. Hadal community structure: implications from the Aleutian Trench. J. Mar. Res. 34 (4), 547–560.

Kao, S.J., Dai, M., Selvaraj, K., Zhai, W., Cai, P., Chen, S.N., et al., 2010. Cyclone-driven deep sea injection of freshwater and heat by hyperpycnal flow in the subtropics. Geophys. Res. Lett. 37 (21). https://doi.org/10.1029/2010GL044893.

Karunadasa, K.S.P., Manoratne, C.H., Pitawala, H.M.T.G.A., Rajapakse, R.M.G., 2019. Thermal decomposition of calcium carbonate (calcite polymorph) as examined by in-situ high-temperature X-ray powder diffraction. J. Phys. Chem. Solids 134, 21–28. https://doi.org/10.1016/j.jpcs.2019.05.023.

Kawamura, K., Sasaki, T., Kanamatsu, T., Sakaguchi, A., Ogawa, Y., 2012. Large submarine landslides in the Japan Trench: a new scenario for additional tsunami generation. Geophys. Res. Lett. 39 (5). https://doi.org/10.1029/2011GL050661.

Kioka, A., Schwestermann, T., Moernaut, J., Ikehara, K., Kanamatsu, T., McHugh, C.M., et al., 2019a. Megathrust earthquake drives drastic organic carbon supply to the hadal trench. Sci. Rep. 9 (1), 1553. https://doi.org/10.1038/s41598-019-38834-x.

Kioka, A., Schwestermann, T., Moernaut, J., Ikehara, K., Kanamatsu, T., Eglinton, T.I., Strasser, M., 2019b. Event stratigraphy in a hadal oceanic trench: the Japan Trench as sedimentary archive recording recurrent giant subduction zone earthquakes and their role in organic carbon export to the deep sea. Front. Earth Sci. 7, 319. https://doi.org/10.3389/feart.2019.00319.

Lamb, A.L., Wilson, G.P., Leng, M.J., 2006. A review of coastal palaeoclimate and relative sea-level reconstructions using δ13C and C/N ratios in organic material. Earth-Sci. Rev. 75 (1–4), 29–57. https://doi.org/10.1016/j.earscirev.2005.10.003.

Leduc, D., Rowden, A.A., Glud, R.N., Wenzhöfer, F., Kitazato, H., Clark, M.R., 2016. Comparison between infaunal communities of the deep floor and edge of the Tonga Trench: possible effects of differences in organic matter supply. Deep-Sea Res., Part 1, Oceanogr. Res. Pap. 116, 264–275. https://doi.org/10.1016/j.dsr.2015.11.003.

Luo, M., Gieskes, J., Chen, L., Scholten, J., Pan, B., Lin, G., Chen, D., 2019. Sources, degradation, and transport of organic matter in the new Britain Shelf-Trench continuum, Papua New Guinea. J. Geophys. Res., Biogeosci., 1–16. https://doi.org/10.1029/2018JG004691.

Luo, M., Gieskes, J., Chen, L., Shi, X., Chen, D., 2017. Provenances, distribution, and accumulation of organic matter in the southern Mariana Trench rim and

slope: implication for carbon cycle and burial in hadal trenches. Mar. Geol. 386, 98–106. https://doi.org/10.1016/j.margeo.2017.02.012.

Luo, M., Glud, R.N., Pan, B., Wenzhöfer, F., Xu, Y., Lin, G., Chen, D., 2018. Benthic carbon mineralization in hadal trenches: insights from in situ determination of benthic oxygen consumption. Geophys. Res. Lett. 45 (6), 2752–2760. https://doi.org/10.1002/2017GL076232.

McHugh, C.M., Kanamatsu, T., Seeber, L., Bopp, R., Cormier, M.-H., Usami, K., 2016. Remobilization of surficial slope sediment triggered by the A.D. 2011 Mw 9 Tohoku-Oki earthquake and tsunami along the Japan Trench. Geology 44 (5), 391–394. https://doi.org/10.1130/G37650.1.

McHugh, C.M., Seeber, L., Rasbury, T., Strasser, M., Kioka, A., Kanamatsu, T., et al., 2020. Isotopic and sedimentary signature of megathrust ruptures along the Japan subduction margin. Mar. Geol. 428, 106283. https://doi.org/10.1016/j.margeo.2020.106283.

McIntyre, C.P., Wacker, L., Haghipour, N., Blattmann, T.M., Fahrni, S., Usman, M., et al., 2017. Online 13C and 14C gas measurements by EA-IRMS–AMS at ETH Zürich. Radiocarbon 59 (03), 893–903. https://doi.org/10.1017/RDC.2016.68.

Migeon, S., Garibaldi, C., Ratzov, G., Schmidt, S., Collot, J.-Y., Zaragosi, S., Texier, L., 2017. Earthquake-triggered deposits in the subduction trench of the North Ecuador/South Colombia margin and their implication for paleoseismology. Mar. Geol. 384, 47–62. https://doi.org/10.1016/j.margeo.2016.09.008.

Molenaar, A., Moernaut, J., Wiemer, G., Dubois, N., Strasser, M., 2019. Earthquake impact on active margins: tracing surficial remobilization and seismic strengthening in a slope sedimentary sequence. Geophys. Res. Lett. 46 (11), 6015–6023. https://doi.org/10.1029/2019GL082350.

Mountjoy, J.J., Howarth, J.D., Orpin, A.R., Barnes, P.M., Bowden, D.A., Rowden, A.A., et al., 2018. Earthquakes drive large-scale submarine canyon development and sediment supply to deep-ocean basins. Sci. Adv. 4 (3). http://advances.sciencemag.org/content/4/3/eaar3748.abstract.

Nunoura, T., Takaki, Y., Hirai, M., Shimamura, S., Makabe, A., Koide, O., et al., 2015. Hadal biosphere: insight into the microbial ecosystem in the deepest ocean on Earth. Proc. Natl. Acad. Sci. 112 (11), E1230–E1236. https://doi.org/10.1073/pnas.1421816112.

Pope, E.L., Talling, P.J., Carter, L., Clare, M.A., Hunt, J.E., 2017. Damaging sediment density flows triggered by tropical cyclones. Earth Planet. Sci. Lett. 458, 161–169. https://doi.org/10.1016/j.epsl.2016.10.046.

Pouderoux, H., Proust, J.-N., Lamarche, G., 2014. Submarine paleoseismology of the northern Hikurangi subduction margin of New Zealand as deduced from Turbidite record since 16 ka. Quat. Sci. Rev. 84, 116–131. https://doi.org/10.1016/j.quascirev.2013.11.015.

Rosenheim, B.E., Day, M.B., Domack, E., Schrum, H., Benthien, A., Hayes, J.M., 2008. Antarctic sediment chronology by programmed-temperature pyrolysis: methodology and data treatment. Geochem. Geophys. Geosyst. 9 (4). https://doi.org/10.1029/2007GC001816.

Sakazaki, T., Kano, Y., Ohmura, J., Hattori, K., 2015. On the severe typhoon attacking Edo region in 1856. Sustain. Humanosphere 11, 64–70 (in Japanese).

Sanchez-Silva, L., López-González, D., Villaseñor, J., Sánchez, P., Valverde, J.L., 2012. Thermogravimetric–mass spectrometric analysis of lignocellulosic and marine biomass pyrolysis. Bioresour. Technol. 109, 163–172. https://doi.org/10.1016/j.biortech.2012.01.001.

Schwestermann, T., Huang, J., Konzett, J., Kioka, A., Wefer, G., Ikehara, K., et al., 2020. Multivariate statistical and multi-proxy constraints on earthquake-triggered sediment remobilization processes in the central Japan Trench. Geochem. Geophys. Geosyst. e2019GC008861. https://doi.org/10.1029/2019GC008861.

Strasser, M., Kopf, A., Abegg, F., Asada, M., Bachmann, A.K., Cuno, P., et al., 2017. Report and preliminary results of R/V SONNE cruise SO251-extreme events archived in the Geologial record of JAPAN's subduction margins (EAGER-JAPAN). In: Berichte, MARUM - Zentrum für Marine Umweltwissenschaften, Fachbereich Geowissenschaften, Universität Bremen 318, 217.

Subt, C., Fangman, K.A., Wellner, J.S., Rosenheim, B.E., 2016. Sediment chronology in Antarctic deglacial sediments: reconciling organic carbon 14 C ages to carbonate 14 C ages using Ramped PyrOx. Holocene 26 (2), 265–273. https://doi.org/10.1177/0959683615608688.

Takada, K., Shishikura, M., Imai, K., Ebina, Y., Goto, K., Koshiya, S., et al., 2016. Distribution and ages of tsunami deposits along the Pacific Coast of the Iwate Prefecture. In: Annual Report on Active Fault and Paleoearthquake Researches, vol. 16, pp. 1–52.

Tsuji, T., Ito, Y., Kido, M., Osada, Y., Fujimoto, H., 2011. Potential tsunamigenic faults of the 2011 off the Pacific coast of Tohoku Earthquake 2 (c), 831–834. https://doi.org/10.5047/eps.2011.05.028.

Turnewitsch, R., Falahat, S., Stehlikova, J., Oguri, K., Glud, R.N., Middelboe, M., et al., 2014. Recent sediment dynamics in hadal trenches: evidence for the influence of higher-frequency (tidal near-inertial) fluid dynamics. Deep-Sea Res., Part 1, Oceanogr. Res. Pap. 90, 125–138. https://doi.org/10.1016/j.dsr.2014.05.005.

Usami, K., Ikehara, K., Kanamatsu, T., Kioka, A., Schwestermann, T., Strasser, M., 2021. The link between upper-slope submarine landslides and mass transport deposits in the hadal trenchs. In: Sassa, K. (Ed.), Understanding and Reducing Landslide Disaster Risk Landslide Disaster Risk. Springer, pp. 361–367.

Wang, S.-L., Burr, G.S., Wang, P.-L., Lin, L.-H., Nguyen, V., 2016. Tracing the sources of carbon in clay minerals: an example from western Taiwan. Quat. Geochronol. 34, 24–32. https://doi.org/10.1016/j.quageo.2016.03.004.

Wenzhöfer, F., Oguri, K., Middelboe, M., Turnewitsch, R., Toyofuku, T., Kitazato, H., Glud, R.N., 2016. Benthic carbon mineralization in hadal trenches: assessment by in situ O2 microprofile measurements. Deep-Sea Res., Part 1, Oceanogr. Res. Pap. 116, 276–286. https://doi.org/10.1016/j.dsr.2016.08.013.

Xiao, W., Xu, Y., Haghipour, N., Montluçon, D.B., Pan, B., Jia, Z., et al., 2020. Efficient sequestration of terrigenous organic carbon in the New Britain Trench. Chem. Geol. 533, 119446. https://doi.org/10.1016/j.chemgeo.2019.119446.